A Decoupled Method for the Roe FDS Scheme in the Reacting Gas Path of FUN3D

Kyle B. Thompson[*] and Peter A. Gnoffo[†]

NASA Langley Research Center, Hampton, VA, 23681-2199

An approach is described for decoupling the species continuity equations from the mixture continuity, momentum, and total energy equations for the Roe flux difference splitting scheme. This decoupling simplifies the implicit system, so that the flow solver can be made significantly more efficient, with very little penalty on overall scheme robustness. Most importantly, the computational cost of the point implicit relaxation is shown to scale linearly with the number of species for the decoupled system, whereas the fully coupled approach scales quadratically. It is shown that solving the implicit system in a decoupled fashion significantly reduces the cost in wall time and memory in comparison to the fully coupled approach. This work lays the foundation for development of an efficient adjoint solution procedure for high speed reacting flow.

Nomenclature

A, A_d, A_m	Jacobian Matrices
a	Speed of sound, m/s
$\mathbf{b}$	Residual vector
c_s	Species s mass fraction
C	Decoupled scheme chemical source term Jacobian
D	Decomposed diagonal Jacobian matrix
dv_1, dv_2, dv_3	Eigenvector components
e_s	Internal energy of species s
E	Total Energy
F'_ρ	Decoupled scheme mixture mass flux
F'_{ρ_s}	Decoupled scheme mass flux of species s
$\mathbf{F}$, $\mathbf{F}'$, $\hat{\mathbf{F}}$	Flux vectors
N_{nodes}	Number of nodes
N_{nz}	Number of non-zero off-diagonal entries in Jacobian
N_{nb}	Number of neighbors around local node
O	Decomposed off-diagonal Jacobian matrix
p	Pressure, N/m^2
$\mathbf{R}$, $\mathbf{L}$	Right and left eigenvectors
R_ρ	Decoupled scheme constraint
$\mathbf{S}$	Face normal vector, m^2
$\mathbf{U}$, $\mathbf{U}'$, $\hat{\mathbf{U}}$	Conservative variable vectors
$\overline{U}$	Normal velocity, m/s^2
u, v, w	Components of velocity, m/s
V	Cell volume, m^3
w	Roe scheme weighting factor
ω	Chemical source term scaling factor
$\hat{\mathbf{V}}$	Decoupled variables vector

---

[*]NASA Pathways Intern, Aerothermodynamics Branch, AIAA Student Member.

[†]Senior Research Engineer, Aerothermodynamics Branch, AIAA Fellow.

American Institute of Aeronautics and Astronautics

$\mathbf{W}$	Chemical source term vector
ρ	Mixture density, kg/m^3
ρ_s	Species s density, kg/m^3
$\lambda_1,\ \lambda_2,\ \lambda_3$	Acoustic and convective eigenvalues
$\lambda^-,\ \lambda^+$	Species flux effective eigenvalues
Λ	Diagonal eigenvalue matrix

Superscript

$n, n+1$	Time level
$R,\ L$	Right and left state quantities
f	Face

I. Introduction

The usability of hypersonic solvers on complex geometries is often limited by the extreme problem size associated with high energy physics. The additional equations required in reacting gas simulations lead to large Jacobians that scale quadratically in size to the number of governing equations. This leads to a significant increase in memory required to store the flux linearizations and the computational cost of the point solver. As reacting gas CFD solvers are used to solve increasingly more complex problems, this onerous quadratic scaling of computational cost and Jacobian size will ultimately surpass the current limits of hardware and time constraints on achieving a flow solution.

The proposed method is based heavily upon the work of Candler et al.,[1] where the quadratic scaling between the cost of solving the implicit system and the addition of species mass equations can be reduced to that of a linear scaling by decoupling the species mass equations from the mixture mass, momentum, and energy equations and solving the two decoupled systems sequentially. In the aforementioned work, the scheme was derived for a modified form of the Steger-Warming flux vector splitting method,[2] whereas the work presented here is derived for the Roe flux difference splitting (FDS) scheme.[3]

A primary motivator for the presented work is to prepare for the implementation of an adjoint capability in a reacting gas solver. This is an extremely challenging problem, and a significant hardship is deriving exact Jacobians for a reacting gas system. A beneficial side effect of decoupling the system is the simplification of deriving exact Jacobians for the Roe flux difference splitting scheme. By decoupling the species equations, the mixture mass, moment, and energy flux Jacobians can be easily derived,[4] using a weighting scheme to correct for the non-uniqueness of the pressure linearization.[5] For the decoupled species fluxes, we derive an exact linearization in the presented work. Future work will include an adjoint-based error estimation capability that leverages these exact linearizations.

II. Background: Fully-Coupled Point Implicit Method

All work presented here is for the inviscid conservation equations, but can be extended to include viscous terms. For an inviscid, multi-species mixture, the governing equations in vector form are:

$$\frac{\partial \mathbf{U}}{\partial t} + \nabla \cdot \mathbf{F} = \mathbf{W} \tag{1}$$

or, in finite volume form:

$$\frac{\partial \mathbf{U}}{\partial t} + \frac{1}{V} \sum_f (\mathbf{F} \cdot \mathbf{S})^f = \mathbf{W} \tag{2}$$

American Institute of Aeronautics and Astronautics

summing over all faces, f, in the domain, with V being the cell volume, $\mathbf{W}$ being the chemical source term vector, and $\mathbf{S}$ being the face outward normal vector. The vectors of conserved variables and fluxes are:

$$\mathbf{U} = \begin{pmatrix} \rho_1 \\ \vdots \\ \rho_{ns} \\ \rho u \\ \rho v \\ \rho w \\ \rho E \end{pmatrix}, \quad \mathbf{F} = \begin{pmatrix} \rho_1 \overline{U} \\ \vdots \\ \rho_{ns} \overline{U} \\ \rho u \overline{U} + p s_x \\ \rho u \overline{U} + p s_y \\ \rho u \overline{U} + p s_z \\ (\rho E + p) \overline{U} \end{pmatrix} \tag{3}$$

Where $\overline{U}$ is the outward pointing normal velocity and ρE is the total energy of the mixture, defined as:

$$E = \sum c_s e_s + \frac{u^2 + v^2 + w^2}{2} \tag{4}$$

where e_s is the internal energy of species s. Using the Roe FDS scheme the numerical fluxes can be expressed as follows:

$$\mathbf{F}^f = \frac{\mathbf{F}(\mathbf{U}^L) + \mathbf{F}(\mathbf{U}^R)}{2} - \frac{1}{2}\mathbf{R} \mid \Lambda \mid \mathbf{L}(\mathbf{U}^R - \mathbf{U}^L) \tag{5}$$

Where Λ is the diagonal eigenvalue matrix, and $\mathbf{R}$ and $\mathbf{L}$ are the right and left eigenvectors, respectively. We now linearize the flux and the source term vectors as:

$$\mathbf{F}^{n+1} \approx \mathbf{F}^n + \frac{\partial \mathbf{F}}{\partial \mathbf{U}} \delta \mathbf{U}^n$$

$$\mathbf{W}^{n+1} \approx \mathbf{W}^n + \frac{\partial \mathbf{W}}{\partial \mathbf{U}} \delta \mathbf{U}^n \tag{6}$$

where $\delta \mathbf{U}^n = \mathbf{U}^{n+1} - \mathbf{U}^n$. Using an implicit time integration, the implicit scheme becomes:

$$\frac{\delta \mathbf{U}^n}{\Delta t} + \frac{1}{V} \sum_f \left(\frac{\partial \mathbf{F}^f}{\partial \mathbf{U}^{\mathbf{L}}} \delta \mathbf{U}^L + \frac{\partial \mathbf{F}^f}{\partial \mathbf{U}^{\mathbf{R}}} \delta \mathbf{U}^R \right)^n \mathbf{S}^f - \frac{\partial \mathbf{W}}{\partial \mathbf{U}} \delta \mathbf{U}^n = -\frac{1}{V} \sum_f (\mathbf{F}^f \cdot \mathbf{S}^f)^n + \mathbf{W}^n \tag{7}$$

or, put more simply:

$$A \delta \mathbf{U}^n = \mathbf{b} \tag{8}$$

where A is the Jacobian matrix of the fully coupled system, and $\mathbf{b}$ is the residual vector. For a point implicit relaxation scheme, the Jacobian matrix can be split into its diagonal and off-diagonal elements, with the latter moved to the RHS as such:

$$A = O + D \tag{9}$$

Each matrix element is a square $(ns+4) \times (ns+4)$ matrix. One method of solving this system is a Red-Black Gauss-Seidel scheme, where matrix coefficients with even indices are updated first and, subsequently, the coefficients with odd indices are updated. This enables better vectorization in solving the linear system. A key point here is the matrix multiplication of the elements of the decomposed A matrix is a quadratic operation; thus, the cost of solving the implicit system scales quadratically with the number of equations being solved. The addition of viscous terms does not change the form of the system.

III. Background: Decoupled Point Implicit Method

By replacing the species mass equations with a single mixture equation and separating the mixture equations from the species mass equations, the conserved variables become:

$$\mathbf{U}' = \begin{pmatrix} \rho \\ \rho u \\ \rho v \\ \rho w \\ \rho E \end{pmatrix} \quad \hat{\mathbf{U}} = \begin{pmatrix} \rho_1 \\ \vdots \\ \rho_{ns} \end{pmatrix} \tag{10}$$

American Institute of Aeronautics and Astronautics

Solving for the flux is now done in two sequential steps. The mixture fluxes are first solved as:

$$\frac{\partial \mathbf{U}'}{\partial t} + \frac{1}{V} \sum_f (\mathbf{F}' \cdot \mathbf{S})^f = 0 \tag{11}$$

Followed by the species fluxes

$$\frac{\partial \hat{\mathbf{U}}}{\partial t} + \frac{1}{V} \sum_f (\hat{\mathbf{F}} \cdot \mathbf{S})^f = \hat{\mathbf{W}} \tag{12}$$

The point relaxation proceeds using Red-Black Gauss-Seidel to update the conserved variables in $\mathbf{U}'$ and all associated auxiliary variables, such as temperature, pressure, speed of sound, etc. This is done holding the thermo-chemical state constant, and will always result in the relaxation of a 5-equation system.

The solution of the species mass equations takes a different form. Based on the work of Candler et al.,[1] the decoupled variables can be rewritten in terms of mass fraction, as follows:

$$\delta \hat{\mathbf{U}}^n = \rho^{n+1} \hat{\mathbf{V}}^{n+1} - \rho^n \hat{\mathbf{V}}^n = \rho^{n+1} \delta \hat{\mathbf{V}}^n + \hat{\mathbf{V}}^n \delta \rho^n \tag{13}$$

where $\hat{\mathbf{V}} = (c_1, \ldots, c_{ns})^T$, and $c_s = \rho_s/\rho$ the mass fraction of species s. While the derivation of the species mass equations is different from that of the Steger-Warming FVS scheme proposed by Candler et al.,[1] the final result takes a similar form:

$$\hat{F}_{\rho_s} = c_s F'_\rho + (c_s^L - \tilde{c}_s)\rho^L \lambda^+ + (c_s^R - \tilde{c}_s)\rho^R \lambda^- \tag{14}$$

where F'_ρ is the total mass flux computed previously using all $\mathbf{U}'$ variables. Likewise, linearizing the species mass fluxes with respect to the $\hat{\mathbf{V}}$ variables yields:

$$\hat{\mathbf{F}}^{n+1} = \hat{\mathbf{F}}^n + \frac{\partial \hat{\mathbf{F}}}{\partial \hat{\mathbf{V}}^L} \delta \hat{\mathbf{V}}^L + \frac{\partial \hat{\mathbf{F}}}{\partial \hat{\mathbf{V}}^R} \delta \hat{\mathbf{V}}^R \tag{15}$$

$$\frac{\partial \hat{\mathbf{F}}}{\partial \hat{\mathbf{V}}^L} = w F_\rho + (1 - w)\rho^L \lambda^+ - w\rho^R \lambda^- \tag{16}$$

$$\frac{\partial \hat{\mathbf{F}}}{\partial \hat{\mathbf{V}}^R} = (1 - w) F_\rho + (w - 1)\rho^L \lambda^+ + w\rho^R \lambda^- \tag{17}$$

A full derivation of Eq.s (14-17), with definition of w and ==the ˜ notation is included in Appendix A.== The chemical source term is evaluated with the $\mathbf{U}'$ variables, and the linearization is carried out as:

$$\hat{\mathbf{W}}^{n+1} = \hat{\mathbf{W}}^n + \left.\frac{\partial \hat{\mathbf{W}}}{\partial \mathbf{U}}\right|_{\mathbf{U}'} \frac{\partial \mathbf{U}}{\partial \hat{\mathbf{V}}} \tag{18}$$

For simplicity of notation, we define:

$$C = \left.\frac{\partial \hat{\mathbf{W}}}{\partial \mathbf{U}}\right|_{\mathbf{U}'} \frac{\partial \mathbf{U}}{\partial \hat{\mathbf{V}}} \tag{19}$$

The decoupled system to be solved becomes:

$$\rho^{n+1} \frac{\delta \hat{\mathbf{V}}^n}{\Delta t} + \frac{1}{V} \sum_f \left(\frac{\partial \hat{\mathbf{F}}^f}{\partial \hat{\mathbf{V}}^L} \delta \hat{\mathbf{V}}^L + \frac{\partial \hat{\mathbf{F}}^f}{\partial \hat{\mathbf{V}}^R} \delta \hat{\mathbf{V}}^R\right)^{n,n+1} \mathbf{S}^f - C^{n,n+1} \delta \mathbf{V}^n$$

$$= -\frac{1}{V} \sum_f (\hat{\mathbf{F}}^{n,n+1} \cdot \mathbf{S})^f + \mathbf{W}^{n,n+1} - \hat{\mathbf{V}}^n \frac{\delta \rho^n}{\Delta t} - R_\rho \tag{20}$$

$$R_\rho = -\frac{1}{V} \sum_f \sum_s (\hat{F}_{\rho_s}^{n,n+1} \cdot \mathbf{S}) \tag{21}$$

where R_ρ is included to preserve the constraint that the mass fractions sum to unity, i.e., $\sum_s c_s = 1$, $\quad \sum_s \delta c_s = 0$.

IV. Cost and Memory Savings of the Decoupled Implicit Problem

In decoupling the species equations, the most significant savings comes from the source term linearization being purely node-based.[6] Solving the mean flow equations is conducted in the same manner as the fully coupled system, where all entries in the Jacobian A_m are 5×5 matrices. For the decoupled implicit system, all entries in the Jacobian A_d are $ns \times ns$ matrices. Because there is no interdependence of species, except through the chemical source term, all contributions due to linearizing the convective flux are purely diagonal $ns \times ns$ matrices. Via Eq. (9), we decompose A_d into its diagonal and off-diagonal elements, resulting in the following linear system:

$$
\begin{pmatrix} \square & & & \\ & \ddots & & \\ & & \square & \\ & & & \ddots \\ & & & & \square \end{pmatrix} \begin{pmatrix} \delta\hat{\mathbf{V}}_1 \\ \vdots \\ \delta\hat{\mathbf{V}}_i \\ \vdots \\ \delta\hat{\mathbf{V}}_{nodes} \end{pmatrix} = \begin{pmatrix} \hat{b}_1 \\ \vdots \\ \hat{b}_i \\ \vdots \\ \hat{b}_{nodes} \end{pmatrix} - \begin{pmatrix} (\sum_{j=1}^{N_{nb}} [\diagdown]\delta\hat{\mathbf{V}}_j)_1 \\ \vdots \\ (\sum_{j=1}^{N_{nb}} [\diagdown]\delta\hat{\mathbf{V}}_j)_i \\ \vdots \\ (\sum_{j=1}^{N_{nb}} [\diagdown]\delta\hat{\mathbf{V}}_j)_{nodes} \end{pmatrix}
\tag{22}
$$

where $\square$ represents a dense $ns \times ns$ matrix, $[\diagdown]$ represents a diagonal matrix, and $\delta\hat{\mathbf{V}}_j$ is the decoupled variable update on the node j that neighbors node i, with N_{nb} being the number of nodes neighboring node i. Thus, the non-zero entries in the off-diagonal matrix can be reduced from diagonal matrices to vectors, reducing the rank of the overall matrix by 1. This results in significant savings in both cost and memory, as the only quadratic operation left in solving the implicit system is dealing with the diagonal entries in the Jacobian. Because the off-diagonal entries significantly outnumber the diagonal entries, we can expect nearly linear scaling in cost with the number of species. Utilizing compressed row storage[7] for the off-diagonal entries, the relative memory savings in the limit of a large number of species for the Jacobian is given by:

$$
\begin{aligned}
Relative\ Memory\ Cost &= \frac{size(A_d)}{size(A)} \\
&= \lim_{ns \to \infty} \frac{(ns^2 + 5^2)(N_{nodes}) + (ns + 5^2)(N_{nz})}{(ns + 4)^2(N_{nodes} + N_{nz})} \\
&= \frac{N_{nodes}}{N_{nodes} + N_{nz}}
\end{aligned}
\tag{23}
$$

Where N_{nodes} is the number of nodes, and N_{nz} is the number of non-zero off-diagonal entries stored using compressed row storage. For a structured grid, each node has 6 neighbors in 3D, i.e., $N_{nz} = 6N_{nodes}$; therefore, we can expect the Jacobian memory required to decrease by a factor of 7 using this decoupled scheme. Interestingly, for a grid that is not purely hexahedral, $N_{nz} > 6N_{nodes}$, making this decoupled scheme even more efficient for unstructured grids than structured grids when using compressed row storage.

V. Results

A. Cylinder

Both the proposed decoupled scheme and the traditional, fully coupled approach have been implemented in the NASA Langley unstructured grid solver FUN3D.[8] To demonstrate the improved efficiency in cost and memory required utilizing the decoupled scheme, and that both the fully coupled and decoupled approaches converge to the same result, a grid convergence study was conducted on a simple cylinder geometry (radius 0.5 m). A 50 x 50, 100 x 100, and 200 x 200 family of grids were adapted using the adaptation capability in FUN3D[9] to produce shock-aligned grids that approximate a true coarsening of the finest grid level. The free stream conditions used were $V_\infty = 5000\ m/s$, $\rho_\infty = 0.001\ kg/m^3$, $T_\infty = 200\ K$. Several chemical kinetics models were used, including a 5-species model with 5 reactions, an 11-species model with 22 reactions, and an 18-species model with 29 reactions.

1. Comparison of Solution

Most important is that the decoupled and fully coupled scheme give nearly identical converged solutions. To quantitatively assess this, we compare the predicted surface pressure, surface temperature, the species

American Institute of Aeronautics and Astronautics

composition on the stagnation line for both schemes. Figure 1 show the predicted quantities on the 100 x 100 grid, for species mixture of N, N_2, O, O_2, and NO, with 5 reactions. All results are indeed nearly identical, with temperature and pressure matching discretely to 8 digits and the species mass fractions on the stagnation line matching to 4 digits. This difference was observed to be reduced slightly more on the finest grid level of 200 x 200.
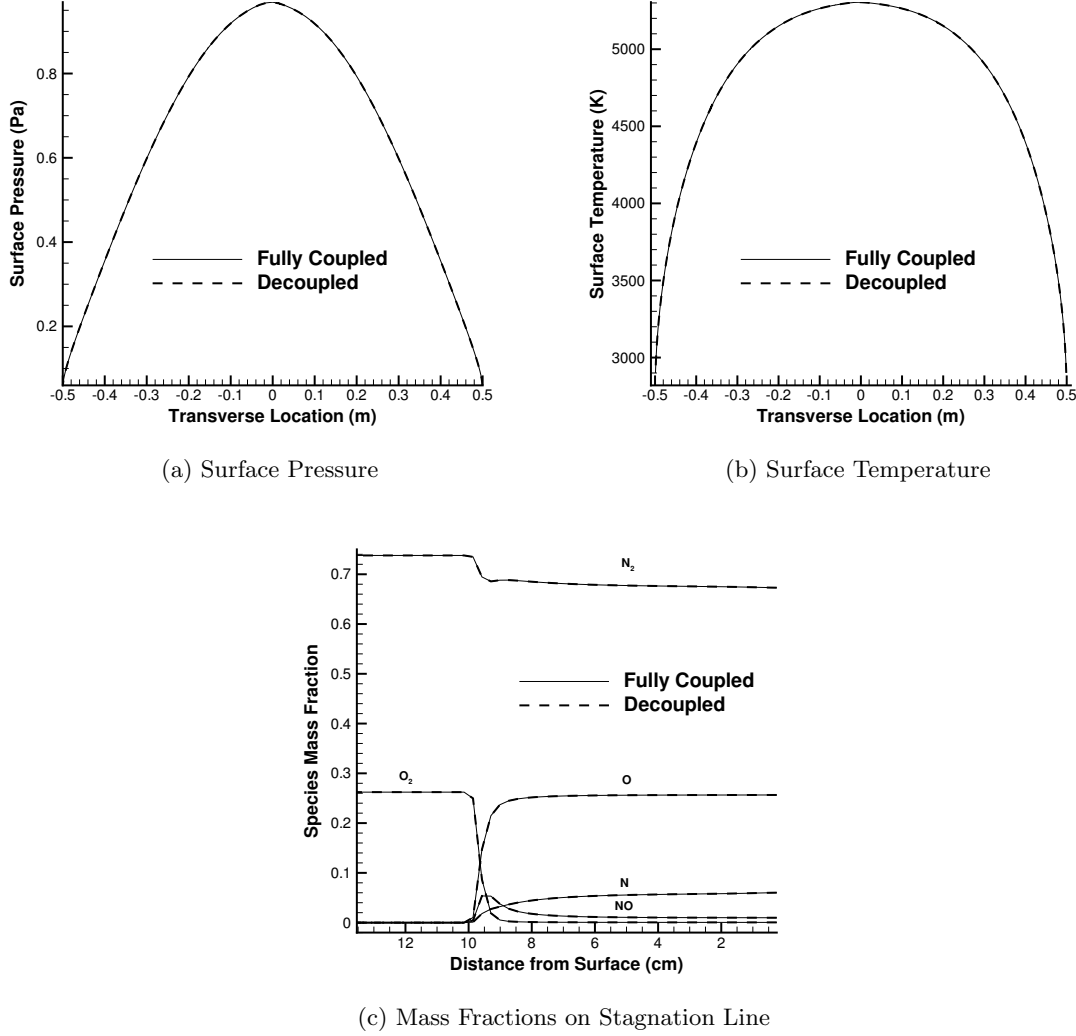

(a) Surface Pressure

(b) Surface Temperature

(c) Mass Fractions on Stagnation Line

Figure 1: Cylinder Predicted Quantities

2. Memory Cost

In order to determine the required memory of the decoupled scheme in comparison to the fully coupled scheme, a convergence study was conducted using Valgrind[10] to determined the memory actually allocated by FUN3D for an increasing number of species. Figure 2 shows the relative memory cost converges asymptotically to ~ 0.25, which is nearly twice the predicted value of 1/7. For the implementation of FUN3D this is actually correct, because the off-diagonal entries are reduced from double precision to single precision. Starting from Eq. (23), for a structured grid (as is the case here) where each node has 6 neighbors, the relative memory cost come to:

$$Relative\ Memory\ Cost = \frac{N_{nodes}}{N_{nodes} + N_{nz}} = \frac{N_{nodes}}{N_{nodes} + (6N_{nodes}/2)} = \frac{1}{4} \tag{24}$$
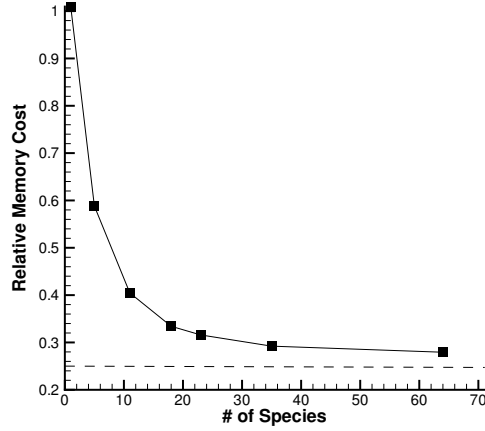
American Institute of Aeronautics and Astronautics

Figure 2: Memory Required Convergence Study

thus, the relative memory saved by using the decoupled scheme correctly approaches a factor of 1/4.

3. Computational Cost

As stated before, the cost of solving the decoupled implicit system should scale approximately linearly with the number of species, whereas the fully coupled problem should scale quadratically; thus, the speedup of the implicit solve should be approximately linear when comparing the decoupled and fully coupled approaches. Figure 3a shows this to be true for the cylinder test case. Figure 3b shows the total speed up of the problem to be less than that of the just the linear solve. This is to be expected, as there are many other factors that scale with the number of species, especially calculating the species source term and its linearization.
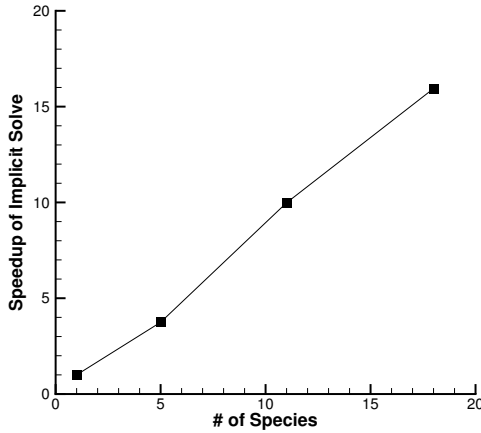
(a) Relative Speedup of Implicit Solve
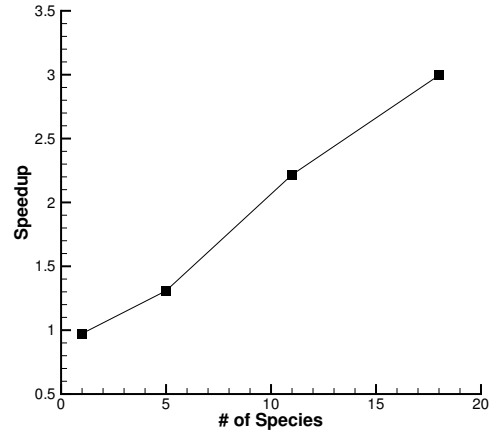
(b) Overall Relative Speedup

Figure 3: Relative Speedup for the Decoupled Scheme vs. Fully Coupled Scheme

B. Sphere-Cone

To ensure that the decoupled scheme is robust and accurate at higher velocities, both the fully coupled and decoupled approaches were run on a sphere-cone geometry identical to that presented by Candler et. al.[1] (10 cm nose radius, 1.1 m length, 8 deg cone angle). For this case, a simple 64x64 grid was constructed, and

American Institute of Aeronautics and Astronautics

freestream conditions were set as $V_\infty = 15000 \; m/s$, $\rho_\infty = 0.001 \; kg/m^3$, $T_\infty = 200 \; K$. It was discovered that CFL limitations for the decoupled scheme were prohibitive, due to the stiffness of the chemical source term. In order to converge the scheme in a manner competitive with the fully coupled approach, it was necessary to scale the magnitude of the source term contribution to the flux balance by a value ω, such that $0 \le \omega \le 1$. To ensure that the decoupled and fully coupled approaches yielded the same result, a ramping scheme was implemented such that no scaling was performed on the source term when solution was in a converged state.

1. Comparison of Results

As with the cylinder test case, the surface pressure and temperature were used as metrics to determine that both the decoupled and fully coupled approaches give the same answer when converged to steady-state. The species composition consisted of N, N_2, O, O_2, NO, N^+, N_2^+, O^+, O_2^+, NO^+, and electrons, with 22 possible reactions. Figure 4 shows that both methods again overplot each other, and the high stagnation temperature is indicative of the fact that this is an inviscid, one-temperature simulation. A benefit of this is that it shows that the decoupled approach is robust enough to converge to the same solution as the fully coupled solution, in spite of the chemical reactions proceeding very rapidly due to a high stagnation temperature.
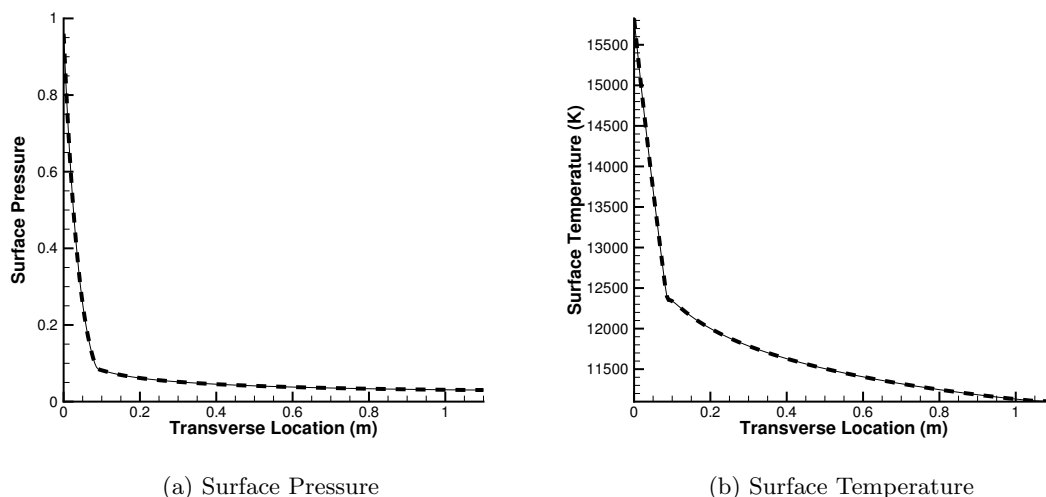

(a) Surface Pressure (b) Surface Temperature

Figure 4: Sphere-Cone Predicted Quantities

2. Convergence Quality

The limits on the stability of the decoupled scheme derives from introducing explicitness in the creating and destruction of chemical species. By ramping the magnitude of the chemical source term, this instability can be mitigated, and the convergence of decoupled scheme approaches that of the fully coupled scheme. Figure 5 shows that the convergence of both schemes progresses nearly identically, with the decoupled scheme converging in significantly less computational time and, interestly, fewer timesteps. This demonstrates that the decoupled scheme has significant potential to improve the effiency of high-velocity simulations, and that the stiffness of the source term is not a debilitating handicap in the presence of large chemical reaction rates.

VI. Conclusion

The motivation for this work was to greatly increase the efficiency of the reacting gas flow solver path in FUN3D to aid in the development of an adjoint development for this path. The work presented here extends the derivation of a decoupled Steger-Warming scheme to that of the Roe FDS scheme, and greatly reduces to the cost of solving the implicit system. Because of the complexity of the high-energy physics and the large problem size associated with additional equations needed to preserve species mass, this increased efficiency is extremely beneficial towards an adjoint formulation. More importantly, the decoupling of the species

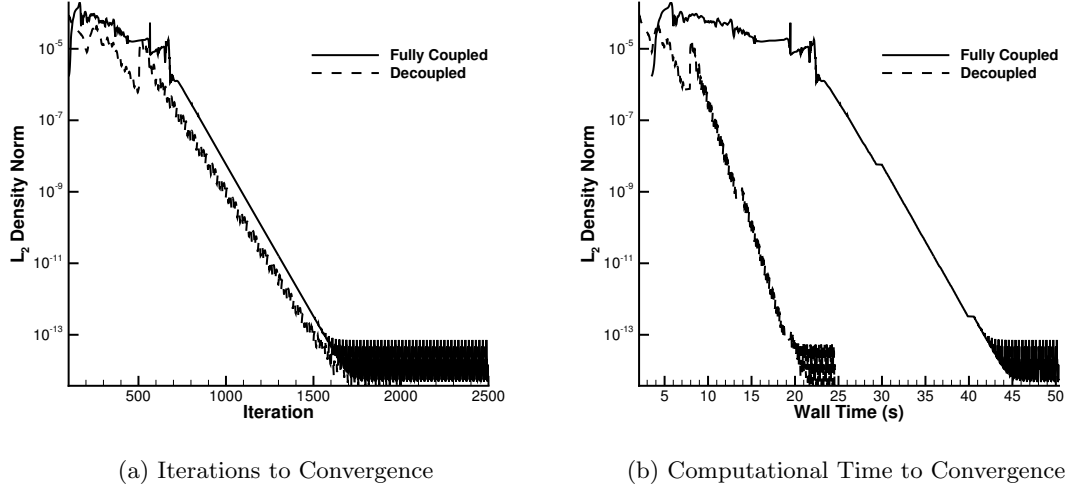(a) Iterations to Convergence

(b) Computational Time to Convergence

Figure 5: Sphere-Cone Convergence Details

equations from the mixture equations presents significant opportunities in obtaining accurate Jacobians for the Roe FDS scheme, which are extremely useful in solving the adjoint problem. The $\sim 300\%$ decrease in memory required and 300% speedup for the 18-species case and the demostrated robustness at very high velocities clearly illustrates significant advantages of this method.

A. Decoupled Flux Derivation

For the Roe Flux Difference Splitting scheme, the species mass fluxes are given by:

$$F_{\rho_s} = \frac{\rho_s^L \overline{U}^L + \rho_s^R \overline{U}^R}{2} - \frac{\tilde{c}_s(\lambda_1 dv_1 + \lambda_2 dv_2) + \lambda_3 dv_{3_s}}{2} \tag{25}$$

$$dv_1 = \frac{p^R - p^L + \tilde{\rho}\tilde{a}(\overline{U}^R - \overline{U}^L)}{\tilde{a}^2} \tag{26}$$

$$dv_2 = \frac{p^R - p^L - \tilde{\rho}\tilde{a}(\overline{U}^R - \overline{U}^L)}{\tilde{a}^2} \tag{27}$$

$$dv_{3_s} = \frac{\tilde{a}^2(\rho_s^R - \rho_s^L) - \tilde{c}_s(p^R - p^L)}{\tilde{a}^2} \tag{28}$$

$$\lambda_1 = \mid \overline{\mathbf{U}} + \tilde{a} \mid, \quad \lambda_2 = \mid \overline{\mathbf{U}} - \tilde{a} \mid, \quad \lambda_3 = \mid \overline{\mathbf{U}} \mid \tag{29}$$

where the ˜ notation signifies a roe-averaged quantity, given by:

$$\tilde{\mathbf{U}} = w\tilde{\mathbf{U}}^L + (1-w)\tilde{\mathbf{U}}^R \tag{30}$$

$$w = \frac{\tilde{\rho}}{\tilde{\rho} + \rho^R} \tag{31}$$

The species mass fluxes must sum to the total mass flux; thus, the total mixture mass flux is given as:

$$F_\rho = \sum_s F_{\rho_s} = \frac{\rho^L \overline{U}^L + \rho^R \overline{U}^R}{2} - \frac{\tilde{c}_s(\lambda_1 dv_1 + \lambda_2 dv_2) + \lambda_3 dv_3}{2} \tag{32}$$

$$dv_3 = \frac{\tilde{a}^2(\rho^R - \rho^L) - (p^R - p^L)}{\tilde{a}^2} \tag{33}$$

Multiplying eq. (32) by the roe-averaged mass fraction and substituting into eq. (25) results in:

$$F_{\rho_s} = \tilde{c}_s F_\rho + \frac{(c_s^L - \tilde{c}_s)\rho^L(\overline{U}^L + |\tilde{U}|)}{2} + \frac{(c_s^R - \tilde{c}_s)\rho^R(\overline{U}^R - |\tilde{U}|)}{2} \tag{34}$$

It should be noted here that the roe-averaged normal velocity, $\tilde{U}$, requires an entropy correction in the presence of strong shocks.[11] This correction has no dependence on the species mass fractions; therefore, it does not change the form of the jacobian for this decoupled scheme. The notation can be further simplified by defining the normal velocities as follows:

$$\lambda^+ = \frac{\overline{U}^L + |\tilde{U}|}{2}, \quad \lambda^- = \frac{\overline{U}^R - |\tilde{U}|}{2} \tag{35}$$

Finally, substituting Eq. (35) into Eq. (34) yields the final result for calculating the species flux in the decoupled system:

$$F_{\rho_s} = \tilde{c}_s F_\rho + (c_s^L - \tilde{c}_s)\rho^L \lambda^+ + (c_s^R - \tilde{c}_s)\rho^R \lambda^- \tag{36}$$

Forming the convective contributions to the Jacobians is straightforward. Because the $\mathbf{U}'$ level variables are constant, only the left, right, and roe-averaged state mass fractions vary. Differentiating Eq. (36) with respect to the mass fraction, c_s, the left and right state contributions are:

$$\frac{\partial F_{\rho_s}}{\partial c_s^L} = w F_\rho + (1-w)\rho^L \lambda^+ - w\rho^R \lambda^- \tag{37}$$

$$\frac{\partial F_{\rho_s}}{\partial c_s^R} = (1-w) F_\rho + (w-1)\rho^L \lambda^+ + w\rho^R \lambda^- \tag{38}$$

Because there is no dependence between species in decoupled convective formulation, the Jacobian block elements are purely diagonal for the convective contributions, of the form:

$$\begin{pmatrix} \frac{\partial F_{\rho_1}}{\partial c_1} & & 0 \\ & \ddots & \\ 0 & & \frac{\partial F_{\rho ns}}{\partial c_{ns}} \end{pmatrix} \tag{39}$$

Acknowledgments

References

[1]Candler, G. V.; Subbareddy, P. K.; and Nompelis, I.: Decoupled Implicit Method for Aerothermodynamics and Reacting Flows. *AIAA Journal*, Vol. 51, no. 5, 2015/04/23 2013, pp. 1245–1254. URL `http://dx.doi.org/10.2514/1.J052070`.

[2]MacCormack, R. W.; and Candler, G. V.: The solution of the Navier-Stokes equations using Gauss-Seidel line relaxation. *Computers and Fluids*, Vol. 17, no. 1, 1989, pp. 135 – 150. URL `http://www.sciencedirect.com/science/article/pii/0045793089900121`.

[3]Roe, P.: Approximate Riemann solvers, parameter vectors, and difference schemes. *Journal of Computational Physics*, Vol. 43, no. 2, 1981, pp. 357 – 372. URL `http://www.sciencedirect.com/science/article/pii/0021999181901285`.

[4]Nishikawa, H.: *Implementing a Real-Gas Roe Solver into* Implementing a Real-Gas Roe Solver into CFL3D. April 2004.

[5]Shuen, J.-S.; Liou, M.-S.; and Leer, B. V.: Inviscid flux-splitting algorithms for real gases with non-equilibrium chemistry. *Journal of Computational Physics*, Vol. 90, no. 2, 1990, pp. 371 – 395. URL `http://www.sciencedirect.com/science/article/pii/002199919090172W`.

[6]Gupta, P. A. G. R. N.; and Shinn, J. L.: Conservation Equations and Physical Models for Hypersonic Air Flows in Thermal and Chemical Nonequilibrium. Tehnical Paper 2867, NASA, 1989.

[7]George, A.; and Liu, J. W.: *Computer Solution of Large Sparse Positive Definite*. Prentice Hall Professional Technical Reference, 1981.

[8]Anderson, W. K.; and Bonhaus, D. L.: "An Implicit Upwind Algorithm for Computing Turbulent Flows on Unstructured Grids". *Computers and Fluids*, Vol. 23, no. 1, 1994, pp. 1–22.

[9]Bartels, R.; Vatsa, V.; Carlson, J.-R.; and Mineck, R.: *FUN3D Grid Refinement and Adaptation Studies for the Ares Launch Vehicle*, American Institute of Aeronautics and Astronautics. 2015/10/06 2010. URL http://dx.doi.org/10.2514/6.2010-4372.

[10]ACM SIGPLAN 2007 Conference on Programing Language Design and Implementation: *How to Shadow Every Byte of Memory Used by a Program*, June 2007.

[11]Harten, A.: High resolution schemes for hyperbolic conservation laws. *Journal of Computational Physics*, Vol. 49, no. 3, 1983, pp. 357 – 393. URL http://www.sciencedirect.com/science/article/pii/0021999183901365.